

Relationship between KRAS mutations and dual time point ^{18}F -FDG PET/CT imaging in colorectal liver metastases

Wujian Mao,^{1,2,3} Jun Zhou,^{1,2,3} He Zhang,^{1,2,3} Lin Qiu,^{1,2,3} Hui Tan,^{1,2,3}
Yan Hu,^{1,2,3} and Hongcheng Shi^{1,2,3} 

¹Shanghai Institute of Medical Imaging, Shanghai 200032, China

²Department of Nuclear Medicine, Zhongshan Hospital, Fudan University, 180 Fenglin Rd, Shanghai 200032, China

³Nuclear Medicine Institute of Fudan University, Shanghai 200032, China

Abstract

Purpose: To investigate the association between metabolic parameters of dual time point ^{18}F -FDG PET/CT imaging and Kirsten rat sarcoma (KRAS) mutation status in colorectal liver metastases (CRLM).

Methods: Forty-nine colorectal cancer patients with 87 liver metastatic lesions were included in this retrospective study. KRAS gene mutation tests were also performed for all the patients. The maximum standardized uptake value (SUV_{\max}) was measured for each hepatic metastatic lesion on both early and delayed scans, and the change of SUV_{\max} (ΔSUV_{\max}) and retention index (RI) were calculated. Uni-variate and multi-variate analyses were employed to determine the relationship between any PET/CT parameters and KRAS mutation status.

Results: Thirty-seven (42.5%) liver metastatic lesions harboring KRAS mutations were identified. The SUV_{\max} of CRLM with KRAS mutation both on early and delayed scans was significantly higher than those with wild-type KRAS (10.7 ± 6.0 vs. 7.8 ± 3.3 , $P = 0.002$; 15.5 ± 10.1 vs. 10.0 ± 4.2 , $P < 0.001$, respectively). Compared with wild-type KRAS CRLM, ΔSUV_{\max} and RI (%) of CRLM with KRAS mutation were also significantly higher than those with wild-type KRAS (4.8 ± 4.7 vs. 2.2 ± 2.0 , $P < 0.001$; 45.3 ± 28.2 vs. 29.6 ± 24.7 , $P = 0.003$, respectively). Multi-variate analyses showed that the SUV_{\max} on both early and delayed scans, ΔSUV_{\max} , and RI (%) were the 4 independent factors to predict CRLM patients harboring KRAS mutations.

Conclusion: The SUV_{\max} on both early and delayed scans, ΔSUV_{\max} , and RI (%) may be the 4 independent

factors to predict CRLM patients harboring KRAS mutations.

Key words: ^{18}F -FDG PET/CT—Dual time-point imaging—Colorectal cancer—Liver metastasis—KRAS

Colorectal cancer (CRC) is the third most common cancer in the world [1]. Colorectal liver metastases (CRLM) has a high incidence and mortality and is the main factor affecting prognosis [2]. Surgery remains the only potentially curative treatment for patients with CRLM, with reported five-year survival rates approximately 50% [3–5]. However, only about 20% of patients presenting with CRLM are candidates for surgery [6]. The anti-epidermal growth factor receptor (EGFR) monoclonal antibodies, such as cetuximab and panitumumab, can specifically bind to the EGFR and can inhibit cell proliferation by blocking ligand binding. Kirsten rat sarcoma (KRAS) gene is well known as predictive markers of resistance to anti-EGFR monoclonal antibodies. Poor response to the anti-EGFR monoclonal antibodies has been revealed in metastatic CRC patients harboring KRAS mutation in several clinical trials [7, 8]. Recent clinical investigations and ongoing studies indicate that immune checkpoint blockade might have potential in the treatment of patients with CRC. Lal et al. showed that RAS mutant tumors predict for a relatively poor immune infiltration and low inhibitory molecule expression [9]. KRAS and NRAS mutant CRC had significantly lowered levels of CD4+ T cells. Thus, tumor micro-environment of RAS mutant tumors stays in relatively immunologically quiescent status and checkpoint blockade may be less efficacious. In addition, the mutants of KRAS have been

indicated as negative prognostic factors in patients with CRC [10]. Approximately 40% of CRC cases present with KRAS mutation [11]. Consequently, identifying KRAS mutation status is essential in the therapeutic management of CRLM.

The current standard of KRAS mutational testing is based on biopsy specimens or surgical resection by invasive procedures. Furthermore, gene tests were usually performed on primary tumor tissue because of the wide use of the endoscopic biopsy. However, there is intra-tumoral heterogeneity within a tumor or discordant between matched primary tumors and liver metastases. It still remains unclear that the evaluation of KRAS mutation status in the primary tumor tissue can precisely reflect the mutation status of the corresponding liver metastasis. Some studies have shown that there was approximately 10%–20% rate of KRAS discordance between primary tumors and paired metastases in CRC [12, 13]. However, Knijn et al. demonstrated a high-level concordance (96.4%) of KRAS mutations status between primary tumors and liver metastases in 305 paired samples [14]. In addition, the KRAS mutation status of biopsy specimens may not sufficiently represent the exact macroscopic status of the entire tumor. To date, a slight difference in the concordance between endoscopic biopsies and resection specimens of CRC was reported [15]. Genomic instability may be a major cause of tumor heterogeneity at both inter- and intratumoral levels [16, 17].

Non-invasive ^{18}F -FDG PET/CT scan is a useful tool for the diagnosis or monitoring treatment response in CRLM. Furthermore, the dual-time point FDG PET/CT scan is more favorable for the detection of liver metastases in patients with CRC [18, 19]. In vitro studies indicated that the glucose transporter-1 (GLUT1) and glucose uptake were consistently upregulated in CRC cells with KRAS mutations [20]. Subsequent in vivo studies have also confirmed the relationship between the glucose metabolism and KRAS mutations and the role of ^{18}F -FDG PET/CT in predicting KRAS mutation status including primary CRC and non-small-cell lung cancer [21, 22]. To our knowledge, few studies were reported to evaluate the usefulness of dual time point PET/CT imaging in predicting KRAS gene mutation status. The purpose of this study is to explore the relationship between PET/CT parameters and KRAS mutations in CRLM. In addition, we further investigate whether the dual time point PET/CT imaging could play a role in predicting KRAS mutation status.

Methods and materials

Patients

We retrospectively reviewed all patients with suspected CRLM underwent ^{18}F -FDG PET/CT in our institution between January 2015 and January 2018. Patients must

meet the following inclusion criteria: (1) Patients underwent a dual-time point ^{18}F -FDG PET/CT scan before surgery/biopsy; (2) The diagnosis of CRLM was proven by pathologic examination; (3) Patients underwent KRAS mutation analysis at the liver metastatic lesions within 1 month after the PET/CT scan; and (4) Patients did not receive any prior therapy, including chemotherapy or radiation therapy, 6 months before PET/CT scans. Moreover, patients with serum glucose level ≥ 150 mg/dL were excluded in this study. Eventually, a total of 49 CRC patients were included and 87 liver metastatic lesions were identified in this retrospective study. This study protocol was approved by the Ethical Review Board of our hospital and the requirement for informed consent was waived due to its retrospective design.

Image acquisition

PET/CT imaging was obtained by following two PET/CT devices: Discovery VCT (GE Healthcare, Milwaukee, Wisconsin, USA) or uMI510 (United Imaging Healthcare, Shanghai, China). All patients fasted for at least 6 h before the PET/CT scan, and blood glucose levels were not greater than 150 mg/dL before the injection. Patients received an intravenous injection approximately 5.1 MBq/kg body weight of ^{18}F -FDG. The PET/CT scan was performed approximately 60 min after ^{18}F -FDG injection. The CT scan parameters were as follows: Discovery VCT (120 mAs; 140 kV; pitch, 0.516; slice thickness, 1.25) or uMI510 (240 mA; 120 kV; pitch, 1.0625; slice thickness, 1.5). A whole-body scan was performed from skull base to mid-thigh with an acquisition time of 2 min per bed position in 3-dimensional mode. The CT images were then reconstructed onto a 512×512 matrix. The PET images were corrected for attenuation correction and reconstructed onto a 128×128 matrix. Delayed scanning only on the upper abdominal cavity approximately 120 min after ^{18}F -FDG injection.

Image analysis

PET/CT results were separately analyzed by two experienced nuclear medicine physicians who were unaware of the mutational status. The standardized uptake value (SUV) was calculated as follows: $\text{SUV} = (\text{decayed corrected activity/tissue volume})/(\text{injected dose/body weight})$. The maximum standardized uptake value (SUV_{max}) was measured for each hepatic metastatic lesion on early and delayed scans ($\text{SUV}_{\text{early}}$ and $\text{SUV}_{\text{delayed}}$, respectively). SUV_{mean} of the normal liver was measured by drawing 3.0 cm sized VOIs three times in the right lobe of normal liver, and the mean value was calculated. In addition, the change of SUV_{max} ($\Delta\text{SUV}_{\text{max}}$) was calculated as $\text{SUV}_{\text{delayed}} - \text{SUV}_{\text{early}}$. Furthermore, reten-

tion index (RI) was calculated as follows: $RI (100\%) = \Delta SUV_{max} \times 100/SUV_{early}$.

Histopathologic analysis

Tissue samples of CRC liver metastases were acquired through biopsy or surgical resection. DNA was extracted from tumor tissue paraffin-embedded sections using the AmoyDx[®] KRAS Mutations Detection Kit (Amoy Diagnostics Co., Ltd., Xiamen, China). KRAS exon 2 (at codon 12 and 13), exon 3 (at codon 61), and exon 4 (at codons 117 and 146) status were amplified by PCR and KRAS mutation was analyzed.

Statistical analysis

All values are presented as mean \pm SD or proportion. PET/CT parameters were compared with KRAS mutation status through Mann–Whitney *U* test. Differences in baseline characteristics between the groups were analyzed by the Chi square test or Mann–Whitney *U* test. Multi-variate logistic regression analysis was performed to analyze the independent predictors of KRAS, and factors with a *P* value of less than 0.10 were included in the model. ROC with calculation of area under the curve (AUC) was used to evaluate their ability to predict mutation status. The DeLong test was used to test for differences in AUC of the ROC. Statistical analyses were performed using SPSS software version 23.0 (IBM Corp., New York, NY, USA; formerly SPSS Inc., Chicago, IL, USA), and ROC curve and the predictive values were estimated using MedCalc Statistical Software version 15.2 (MedCalc Software bvba, Ostend, Belgium). All *P* values are two-sided and values of less than 0.05 were considered to indicate a statistically significant difference.

Results

Patients and tumor characteristics

The study consisted of 49 CRC patients with 87 liver metastases. Seventy-eight (89.7%) tissue samples of liver metastases were obtained from surgical resections, and nine tissue samples (10.3%) were obtained from biopsies. KRAS mutations were identified in 37 (42.5%) liver metastases (exon 2: 28, exon 3: 5, exon 4: 4), while 50 (57.5%) liver metastases were considered as wild-type. SUV_{max} on early and delayed scans of the CRLM were 9.0 ± 4.9 and 12.3 ± 7.8 , respectively. ΔSUV_{max} and RI (%) on dual-time point imaging of CRLM were 3.3 ± 3.6 and 36.2 ± 27.2 , respectively. The characteristics of patients and tumor are summarized in Table 1.

Table 1. Baseline characteristics of 49 patients with 87 liver metastases

Characteristic	Patients	Liver metastases
Age (years)		
≤ 60	18	30
> 60	31	57
Gender		
Male	36	60
Female	13	27
Blood glucose (mmol/L)	5.5 ± 0.7	5.6 ± 0.9
CEA (ng/mL)		
< 5.0	9	12
≥ 5.0	40	75
Primary site of colorectal cancer		
Colon	29	53
Rectum	20	34
Temporal relationship to primary		
Synchronous	13	30
Metachronous	36	57
No. of CRLM		
1	27	
2	13	
3	4	
4	3	
5	2	
Size of CRLM (mm)		28.9 ± 20.5
Histological grade of CRLM		
Well differentiated		31
Moderately differentiated		44
Poorly differentiated		8
Unknown		4
KRAS status of CRLM		
Wild type		50
Mutant		37

CEA, carcinoembryonic antigen

Correlation between metabolic parameters and KRAS mutation status

Uni-variate analysis demonstrated that the SUV_{max} on early and delayed scans were exhibited about a 1.37-fold and 1.55-fold higher in CRLM with mutated KRAS than those with wild-type KRAS ($P = 0.002$ and $P < 0.001$, respectively; Fig. 1A, B). Compared with wild-type KRAS CRLM, ΔSUV_{max} and RI (%) on dual-time point imaging were also showed about a 2.18-fold and 1.53-fold higher in CRLM with KRAS mutation ($P < 0.001$ and $P = 0.012$, respectively; Fig. 1C, D). No significant differences were found between KRAS mutation and wild-type in terms of gender ($P = 0.821$), age ($P = 0.086$), blood glucose level ($P = 0.280$), serum carcinoembryonic antigen (CEA) level ($P = 0.488$), tumor size ($P = 0.372$), histological grade of CRLM ($P = 0.672$), SUV_{mean} of normal liver on early scan ($P = 0.409$), and SUV_{mean} of normal liver in delayed scan ($P = 0.853$). These results are presented in Table 2. The dual-time point PET/CT images in a patient with mutated KRAS and wild-type KRAS are presented in Figs. 2 and 3 respectively. Multi-variate analysis indicated that the SUV_{early} , $SUV_{delayed}$, ΔSUV_{max} and RI (%) were the 4 independent factors to predict CRLM

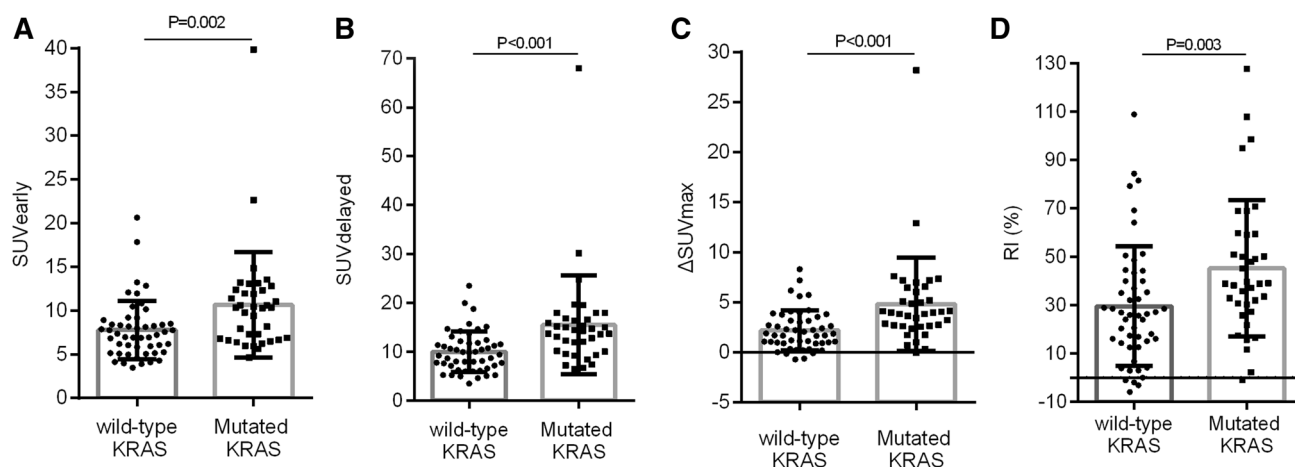


Fig. 1. Distribution of SUV_{early} (A), $SUV_{delayed}$ (B), ΔSUV_{max} (C) and RI (D) according to the status of KRAS.

Table 2. Univariate analysis of factors associated with KRAS status

Factor	Wild-type KRAS (n = 50)	Mutated KRAS (n = 37)	P value
Gender			0.821
Male	34	26	
Female	16	11	
Age (years)			0.086
≤ 60	21	9	
> 60	29	28	
Blood glucose (mmol/L)	5.8 ± 1.0	5.4 ± 0.9	0.280
CEA (ng/mL)			0.488
< 5	8	4	
≥ 5	42	33	
Tumor size (mm)	32.4 ± 25.1	27.2 ± 14.2	0.372
Histological grade of CRLM			0.672
WD + MD	41	34	
PD	5	3	
SUV_{mean} of normal liver (early scan)	2.5 ± 0.3	2.4 ± 0.2	0.409
SUV_{mean} of normal liver (delayed scan)	1.9 ± 0.3	1.8 ± 0.2	0.853
SUV_{early}	7.8 ± 3.3	10.7 ± 6.0	0.002
$SUV_{delayed}$	10.0 ± 4.2	15.5 ± 10.1	< 0.001
ΔSUV_{max}	2.2 ± 2.0	4.8 ± 4.7	< 0.001
RI (%)	29.6 ± 24.7	45.3 ± 28.2	0.003

CEA, carcinoembryonic antigen; WD, well differentiated; MD, moderately differentiated; PD, poorly differentiated; SUV_{early} , SUV_{max} of early scan; $SUV_{delayed}$, SUV_{max} of delayed scan; ΔSUV_{max} , The change of SUV_{max} ; RI (%), Retention Index

patients harboring KRAS mutations. These results are presented in Table 3.

Prediction of KRAS mutation status

ROC analysis showed that the AUC of SUV_{early} , $SUV_{delayed}$ were 0.694 ($P = 0.002$, 95% CI 0.582–0.807) and 0.760 ($P < 0.001$, 95% CI 0.658–0.862), respectively. The AUC of ΔSUV_{max} and RI (%) were 0.757 ($P < 0.001$, 95% CI 0.654–0.861) and 0.684 ($P = 0.003$, 95% CI 0.571–0.797), respectively. The results of the ROC analysis are shown in Fig. 4. $SUV_{delayed}$ was the parameter with the highest AUC among the 4 parameters and presented a sensitivity, specificity, and accuracy of 73.0%, 76.0%, and 74.7%, respectively, for an optimal cut-off of 11.8. The AUC of ΔSUV_{max} and $SUV_{delayed}$

was very close. When the ΔSUV_{max} cut-off value was set at 2.3, the sensitivity, specificity, and accuracy were 83.8%, 62.0% and 71.3% respectively. All the predictive performances of PET/CT parameters results are presented in Table 4.

Pair-wise comparison of the ROC curves was performed to compare the clinical significance of the 4 parameters in predicting KRAS mutation status. On single-phase images, the diagnostic performance of SUV_{max} for the prediction of KRAS status on the delayed scan images was significantly better than that on the early scan images (AUC: 0.760 vs. 0.694, $P = 0.033$). On dual-phase images, the diagnostic performance of ΔSUV_{max} for the prediction of KRAS status was significantly better than RI (AUC: 0.757 vs. 0.684, $P = 0.008$). There were no significant differences in

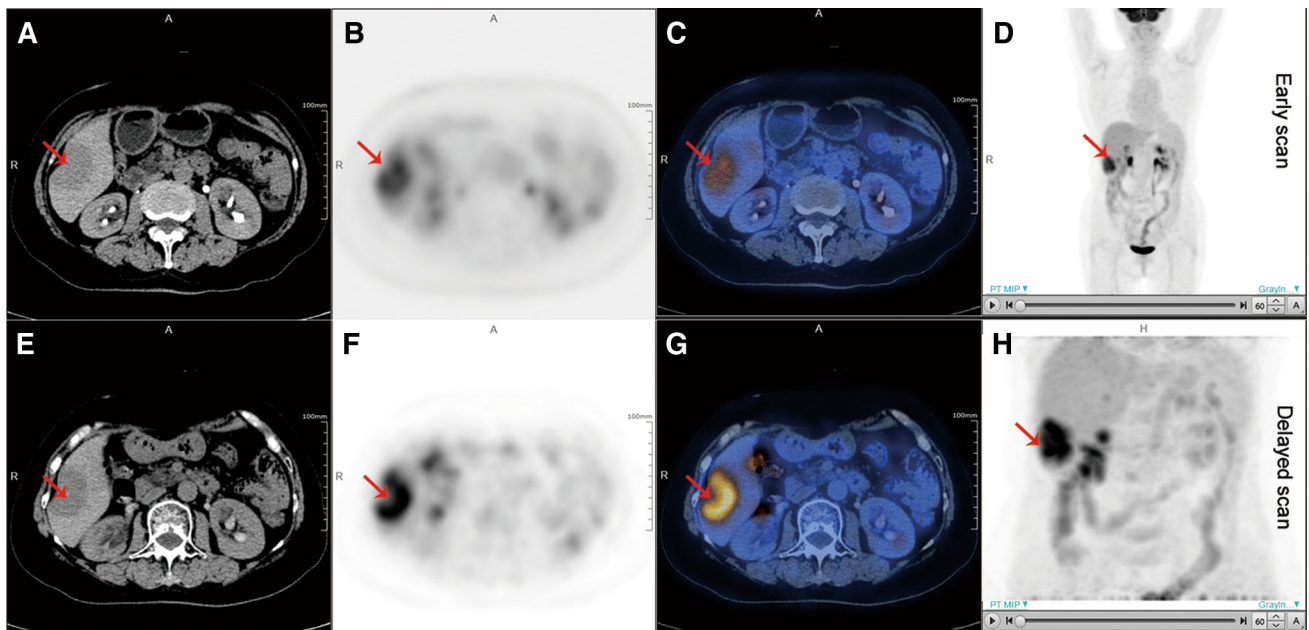


Fig. 2. Representative cases of CRLM harboring wild-type KRAS: A 70 years old woman had 1 liver metastasis (arrow; diameter, 41.7 mm) with wild-type KRAS. The early FDG PET/CT images (A–D) shows intense accumulation ($SUV_{max} = 8.25$). The delayed FDG PET/CT images (E–

H) demonstrates more FDG uptake of the hepatic metastatic lesion ($SUV_{max} = 10.64$). The changes of SUV_{max} and retention index on dual-time point imaging of CRLM were 2.39 and 29% respectively.

Table 3. Multivariate analysis of KRAS status in CRLM ($n = 87$)

Factor	OR	95% CI	<i>P</i> value
Age	1.57	0.58–4.28	0.377
SUV_{early}	1.18	1.02–1.36	0.024
Age	1.32	0.46–3.77	0.602
$SUV_{delayed}$	1.22	1.08–1.38	0.001
Age	1.82	0.66–5.00	0.246
ΔSUV_{max}	1.49	1.17–1.88	0.001
Age	2.29	0.86–6.08	0.097
RI	10.27	1.66–63.51	0.012

OR, odds ratio; CI, confidence interval; SUV_{early} , SUV_{max} of early scan; $SUV_{delayed}$, SUV_{max} of delayed scan; ΔSUV_{max} , The change of SUV_{max} ; RI (%), Retention Index

predicting KRAS status between the $SUV_{delayed}$ and ΔSUV_{max} (AUC: 0.760 vs. 0.757, $P = 0.946$).

Discussion

Recently, the American Society of Clinical Oncology suggests that anti-EGFR monoclonal antibodies are recommended only for metastatic CRC patients with wild-type KRAS [23]. KRAS mutation evaluation is an essential process in patients with CRLM. The current standard of KRAS mutational testing is mainly based on the histopathologic analysis. However, such histologic examination is often limited by tumor heterogeneity, discordance of KRAS mutational status, availability of tumor tissue, and inadequate sampling. This study

demonstrated that the 4 metabolic parameters (SUV_{early} , $SUV_{delayed}$, ΔSUV_{max} , and RI) derived from dual-time point FDG PET/CT imaging were strongly associated with the KRAS mutation status and might be powerfully predictive factors for identifying KRAS mutations in CRLM.

Several studies have indicated a positive correlation between the ¹⁸F-FDG uptake and KRAS mutations in primary CRC [21, 24–27]. However, the specimens of primary CRC for KRAS mutational testing are always readily available because of the wide use of the endoscopic biopsy. Prediction of mutational status of metastasis is consequently a real practical relevance to tumor precision treatment. Accordingly, we investigated the relationship between ¹⁸F-FDG accumulation with KRAS mutations in CRLM. Our study demonstrated that ¹⁸F-FDG uptake in CRLM harboring KRAS mutations was significantly higher than that in wild-type KRAS. Our study results were concordant with the results of Kawada et al. [28]. They showed that CRC metastatic lesions harboring mutated KRAS exhibited about a 1.45 fold increase in SUV_{max} in tumors larger than 10 mm ($P = 0.03$). However, there was no significant difference when the smaller lesions were included in Kawada's study. They interpreted that this bias may be produced by partial volume effect. But this bias does not appear in our study. One possible reason for this discrepancy may be because almost all of the tumors (97.7%) in our study are larger than 10 mm. When the

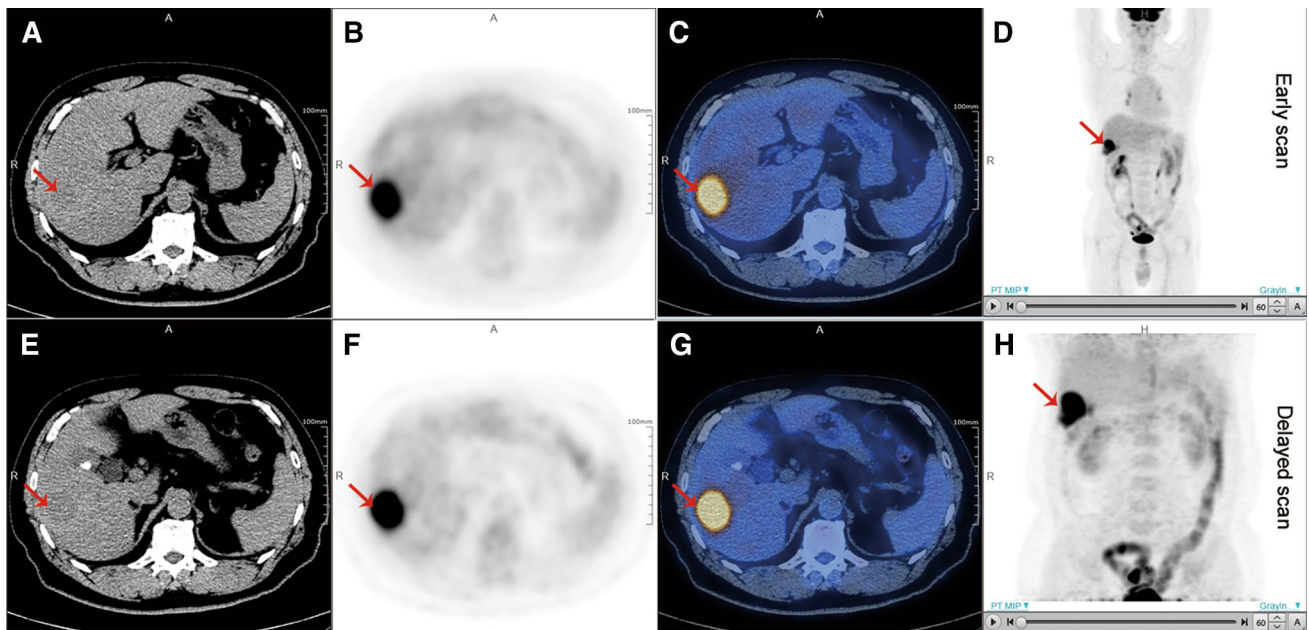


Fig. 3. Representative cases of CRLM harboring mutated KRAS: A 77 years old man had 1 liver metastasis (arrow; diameter, 43.0 mm) with mutated KRAS. The early FDG PET/CT images (A–D) shows intense accumulation ($\text{SUV}_{\text{max}} = 13.13$). The delayed FDG PET/CT images (E–H) demonstrates

more FDG uptake of the hepatic metastatic lesion ($\text{SUV}_{\text{max}} = 19.7$). The changes of SUV_{max} and retention index on dual time point imaging of CRLM were 6.57 and 50% respectively.

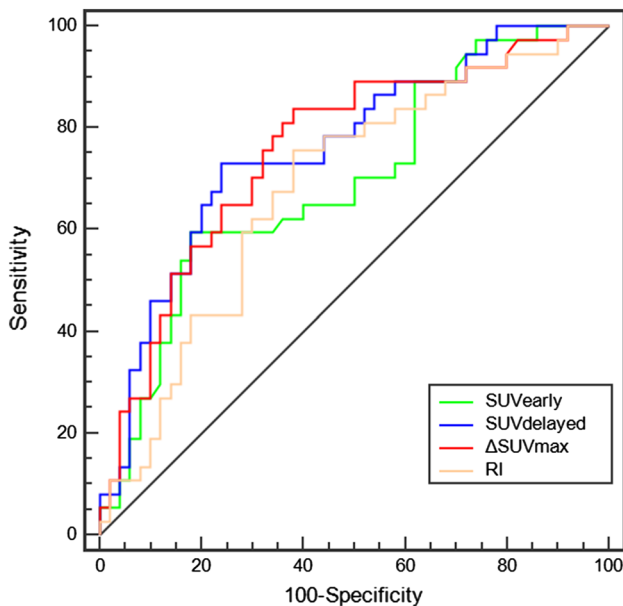


Fig. 4. Receiver operating characteristic curves of $\text{SUV}_{\text{early}}$, $\text{SUV}_{\text{delayed}}$, $\Delta\text{SUV}_{\text{max}}$, and RI for KRAS Mutation prediction.

optimal cut-off value of SUV_{max} was 6.0, KRAS status of metastatic CRC could be predicted with an accuracy of 71.4%. In contrast to our study, Krikelis et al. [29] found that no significant association between SUV_{max} value and KRAS mutations in Caucasian metastatic CRC. And there was also no relationship found between

GLUT1 levels and SUV_{max} . However, SUV_{max} was measured in metastatic lesions, whereas the KRAS status and GLUT1 mRNA levels were tested in the corresponding primary tumors. Consequently, the study might be biased because of discordant KRAS status between primary CRC and its paired metastases. In addition, metastatic lesions were also not confirmed by pathology.

To date, the clinical significance of $\Delta\text{SUV}_{\text{max}}$ and RI derived from dual time point imaging still remains elusive. Some studies have shown that high RI might reflect the high biological aggressiveness of the tumor, and might be related to poor prognosis [30–34]. Our results showed that $\Delta\text{SUV}_{\text{max}}$ and RI on dual-time point ^{18}F -FDG PET/CT imaging were significantly higher in CRLM with mutated KRAS than those with wild-type KRAS. This is consistent with the finding that KRAS mutation was associated with poorer prognosis in patients with CRC [10]. Unfortunately, in our study, the relationship between KRAS mutation and the survival was not investigated. There were few reports on the relationship between RI and gene status or its expression in primary CRC or CRLM. Lee et al. [35] showed that the higher RI had a significant correlation with larger tumor size, higher T staging, higher GLUT-1 expression, and higher p53 expression in primary CRC. Our results and previous investigations presumed that $\Delta\text{SUV}_{\text{max}}$ and RI might have the potential to be applied as a prognostic marker in primary CRC and CRLM.

Table 4. The predictive performances of PET/CT parameters in predicting KRAS status

Parameter	AUC	Cut-off value	Sensitivity (%)	Specificity (%)	Accuracy (%)	NPV (%)	PPV (%)
SUV _{early}	0.694	9.2	59.5	82.0	72.4	71.0	73.2
SUV _{delayed}	0.760	11.8	73.0	76.0	74.7	69.2	79.2
ΔSUV _{max}	0.757	2.3	83.8	62.0	71.3	62.0	83.8
RI (%)	0.684	29.0	53.3	86.4	72.3	74.4	71.4

AUC, area under the curve; SUV_{early}, SUV_{max} of early scan; SUV_{delayed}, SUV_{max} of delayed scan; ΔSUV_{max}, The change of SUV_{max}; RI (%), Retention Index; NPV, negative predictive value; PPV, positive predictive value

In our study, PET parameters obtained from dual-time point FDG PET/CT imaging may be a promising imaging biomarker for non-invasively predicting KRAS mutational status in CRLM with an optimal accuracy 74.7%. Prior studies have shown that the overall accuracy of SUV_{max} alone for the prediction of KRAS status of primary CRC was ranging from 50% to 75% [21, 24–26]. Thus, together with previous studies, the overall accuracy of PET/CT parameters was not high enough to be used as clinical index for the prediction of KRAS status in primary CRC and CRLM. Currently, we think ¹⁸F-FDG PET/CT may complement rather than replace molecular testing. Our results also suggested that there was a trend to SUV_{delayed} and ΔSUV_{max} perform better than SUV_{early} and RI. The dual-time point scan might be a feasible way to improve the diagnostic ability of KRAS mutation prediction.

To the best of our knowledge, this is a novel study evaluate the usefulness of dual time point PET/CT imaging in predicting KRAS gene mutation status. There were some limitations in our study. First, it was a retrospective study, with a relatively small sample size. Further a larger, prospective cohort studies will be required. Second, 10.3% of the tissue samples in our study were obtained from biopsies. Therefore, the correlation study might be biased because the KRAS mutation status of biopsy specimens may not sufficiently represent the exact macroscopic status of the entire tumor. Third, the relationship between dual time point ¹⁸F-FDG PET/CT and survival was not evaluated in our analysis. And the clinical impact of PET/CT parameters and KRAS mutation in EGFR therapy response was also not investigated in our analysis. Overall, the current work is an initial attempt to provide a novel approach to KRAS identification and need further exploring in the future.

Conclusion

In conclusion, SUV_{early}, SUV_{delayed}, ΔSUV_{max}, and RI (%) may be the 4 imaging biomarkers to predict CRLM patients harboring KRAS mutations. And SUV_{delayed} and ΔSUV_{max} may be of greater potential for the KARS mutation prediction.

Acknowledgements We thank Dr. Yingjie Zheng for his assistance in statistical analysis.

Compliance with ethical standards

Funding No internal or external grant funds supported this work.

Conflict of interest The authors declare that there is no conflict of interests.

Ethical approval All procedures performed in studies involving human participants were in accordance with the ethical standards of the institutional and/or national research committee and with the 1964 Helsinki declaration and its later amendments or comparable ethical standards.

Informed consent The institutional review board approved this retrospective study. Informed consent was waived.

References

1. Torre LA, Bray F, Siegel RL, et al. (2015) Global cancer statistics. *CA Cancer J Clin* 65(2):87–108
2. Helling TS, Martin M (2014) Cause of death from liver metastases in colorectal cancer. *Ann Surg Oncol* 21(2):501–506
3. Nordlinger B, Sorbye H, Glimelius B, et al. (2013) Perioperative FOLFOX4 chemotherapy and surgery versus surgery alone for resectable liver metastases from colorectal cancer (EORTC 40983): long-term results of a randomised, controlled, phase 3 trial. *Lancet Oncol* 14(12):1208–1215
4. Nanji S, Cleary S, Ryan P, et al. (2013) Up-front hepatic resection for metastatic colorectal cancer results in favorable long-term survival. *Ann Surg Oncol* 20(1):295–304
5. House MG, Ito H, Gonen M et al. (2010) Survival after hepatic resection for metastatic colorectal cancer: trends in outcomes for 1600 patients during two decades at a single institution. *J Am Coll Surg* 210 (5):744–752, 752–745.
6. Kopetz S, Chang GJ, Overman MJ, et al. (2009) Improved survival in metastatic colorectal cancer is associated with adoption of hepatic resection and improved chemotherapy. *J Clin Oncol* 27(22):3677–3683
7. Douillard JY, Oliner KS, Siena S, et al. (2013) Panitumumab-FOLFOX4 treatment and RAS mutations in colorectal cancer. *N Engl J Med* 369(11):1023–1034
8. Karapetis CS, Khambata-Ford S, Jonker DJ, et al. (2008) K-ras mutations and benefit from cetuximab in advanced colorectal cancer. *N Engl J Med* 359(17):1757–1765
9. Lal N, Beggs AD, Willcox BE, et al. (2015) An immunogenomic stratification of colorectal cancer: implications for development of targeted immunotherapy. *Oncoimmunology* 4(3):e976052
10. Kwak MS, Cha JM, Yoon JY, et al. (2017) Prognostic value of KRAS codon 13 gene mutation for overall survival in colorectal cancer: direct and indirect comparison meta-analysis. *Medicine (Baltimore)* 96(35):e7882
11. Neumann J, Zeindl-Eberhart E, Kirchner T, et al. (2009) Frequency and type of KRAS mutations in routine diagnostic analysis of metastatic colorectal cancer. *Pathol Res Pract* 205(12):858–862
12. Voutsina A, Tzardi M, Kalikaki A, et al. (2013) Combined analysis of KRAS and PIK3CA mutations, MET and PTEN expression in primary tumors and corresponding metastases in colorectal cancer. *Mod Pathol* 26(2):302–313
13. Kim MJ, Lee HS, Kim JH, et al. (2012) Different metastatic pattern according to the KRAS mutational status and site-specific discor-

- dance of KRAS status in patients with colorectal cancer. *BMC Cancer* 12:347
14. Knijn N, Mekenkamp LJ, Klomp M, et al. (2011) KRAS mutation analysis: a comparison between primary tumours and matched liver metastases in 305 colorectal cancer patients. *Br J Cancer* 104(6):1020–1026
 15. Krol LC, Hart NA, Methorst N, et al. (2012) Concordance in KRAS and BRAF mutations in endoscopic biopsy samples and resection specimens of colorectal adenocarcinoma. *Eur J Cancer* 48(7):1108–1115
 16. Burrell RA, McGranahan N, Bartek J, et al. (2013) The causes and consequences of genetic heterogeneity in cancer evolution. *Nature* 501(7467):338–345
 17. Gutenber A, Gerdes JS, Jung K, et al. (2010) High chromosomal instability in brain metastases of colorectal carcinoma. *Cancer Genet Cytogenet* 198(1):47–51
 18. Lee JW, Kim SK, Lee SM, et al. (2011) Detection of hepatic metastases using dual-time-point FDG PET/CT scans in patients with colorectal cancer. *Mol Imaging Biol* 13(3):565–572
 19. Dirisamer A, Halpern BS, Schima W, et al. (2008) Dual-time-point FDG-PET/CT for the detection of hepatic metastases. *Mol Imaging Biol* 10(6):335–340
 20. Yun J, Rago C, Cheong I, et al. (2009) Glucose deprivation contributes to the development of KRAS pathway mutations in tumor cells. *Science* 325(5947):1555–1559
 21. Kawada K, Nakamoto Y, Kawada M, et al. (2012) Relationship between ¹⁸F-fluorodeoxyglucose accumulation and KRAS/BRAF mutations in colorectal cancer. *Clin Cancer Res* 18(6):1696–1703
 22. Caicedo C, Garcia-Velloso MJ, Lozano MD, et al. (2014) Role of [(1)(8)F]FDG PET in prediction of KRAS and EGFR mutation status in patients with advanced non-small-cell lung cancer. *Eur J Nucl Med Mol Imaging* 41(11):2058–2065
 23. Allegra CJ, Jessup JM, Somerfield MR, et al. (2009) American Society of Clinical Oncology provisional clinical opinion: testing for KRAS gene mutations in patients with metastatic colorectal carcinoma to predict response to anti-epidermal growth factor receptor monoclonal antibody therapy. *J Clin Oncol* 27(12):2091–2096
 24. Chen SW, Chiang HC, Chen WT, et al. (2014) Correlation between PET/CT parameters and KRAS expression in colorectal cancer. *Clin Nucl Med* 39(8):685–689
 25. Lovinfosse P, Koopmansch B, Lambert F, et al. (2016) ¹⁸F-FDG PET/CT imaging in rectal cancer: relationship with the RAS mutational status. *Br J Radiol* 89(1063):20160212
 26. Lee JH, Kang J, Baik SH, et al. (2016) Relationship between ¹⁸F-fluorodeoxyglucose uptake and V-Ki-Ras2 Kirsten Rat sarcoma viral oncogene homolog mutation in colorectal cancer patients: variability depending on C-reactive protein level. *Medicine (Baltimore)* 95(1):e2236
 27. Cho A, Jo K, Hwang SH, et al. (2017) Correlation between KRAS mutation and ¹⁸F-FDG uptake in stage IV colorectal cancer. *Abdom Radiol (NY)* 42(6):1621–1626
 28. Kawada K, Toda K, Nakamoto Y, et al. (2015) Relationship between ¹⁸F-FDG PET/CT scans and KRAS mutations in metastatic colorectal cancer. *J Nucl Med* 56(9):1322–1327
 29. Krikelis D, Skoura E, Kotoula V, et al. (2014) Lack of association between KRAS mutations and F-¹⁸-FDG PET/CT in caucasian metastatic colorectal cancer patients. *Anticancer Res* 34(5):2571–2579
 30. Abgral R, Valette G, Robin P, et al. (2016) Prognostic evaluation of percentage variation of metabolic tumor burden calculated by dual-phase ¹⁸F FDG PET-CT imaging in patients with head and neck cancer. *Head Neck* 38(Suppl 1):E600–606
 31. Xi Y, Guo R, Hu J, et al. (2014) ¹⁸F-fluoro-2-deoxy-D-glucose retention index as a prognostic parameter in patients with pancreatic cancer. *Nucl Med Commun* 35(11):1112–1118
 32. Garcia Vicente AM, Castrejon AS, Relea Calatayud F, et al. (2012) ¹⁸F-FDG retention index and biologic prognostic parameters in breast cancer. *Clin Nucl Med* 37(5):460–466
 33. Shimizu K, Okita R, Saisho S, et al. (2015) Clinical significance of dual-time-point ¹⁸F-FDG PET imaging in resectable non-small cell lung cancer. *Ann Nucl Med* 29(10):854–860
 34. Houseni M, Chamroonrat W, Zhuang J, et al. (2010) Prognostic implication of dual-phase PET in adenocarcinoma of the lung. *J Nucl Med* 51(4):535–542
 35. Lee JH, Lee WA, Park SG, et al. (2012) Relationship between dual-time point FDG PET and immunohistochemical parameters in preoperative colorectal cancer: preliminary study. *Nucl Med Mol Imaging* 46(1):48–56